The MYC antagonist MNT autoregulates its expression and supports proliferation in MAX deficient cells

M Carmen Lafita-Navarro[1,4], Judit Liaño-Pons[1], Andrea Quintanilla[1,5], Ignacio Varela[1], Fabiana Ourique[1,6], Gabriel Bretones[1,7], Rosa Blanco[1], Julia Aresti[1], Patrick Carroll[2], Peter Hurlin[3], Robert N. Eisenman[2], M. Dolores Delgado[1] and Javier León[1*]

[1]Instituto de Biomedicina y Biotecnología de Cantabria (IBBTEC), Universidad de Cantabria-CSIC, and Department of Molecular Biology, Universidad de Cantabria, Santander, Spain

[2]Division of Basic Sciences, Fred Hutchinson Cancer Research Center, Seattle, USA.

[3]Shriners Hospitals for Children Research Center, and Department of Cell, Developmental and Cancer Biology, Knight Cancer Institute, Oregon Health and Science University, Portland, USA.

[4]Present address: Sorrell lab, Department of Cell Biology UT Southwestern Medical Center, Dallas, USA

[5]Present address: Edinburgh Cancer Research UK Centre, Institute of Genetics and Molecular Medicine, University of Edinburgh, United Kingdom

[6]Present address: Department of Biochemistry, Universidade Federal de Santa Catarina (UFSC), Florianópolis, Brazil

[7]Present address: Departamento de Bioquímica y Biología Molecular, Facultad de Medicina, Instituto Universitario de Oncología (IUOPA), Universidad de Oviedo, Spain

*Corresponding author

Running title: MNT functions in the absence of MAX

Key words: MNT, MAX, MYC, MLX, transcription, promoter

ABSTRACT

MNT is a transcription factor of the MXD family. MNT-MAX dimers down-regulate genes by binding to E-box sequences, which can also be bound by MYC-MAX to activate transcription. MNT has been described as a modulator of MYC activity but little is known about MNT regulation and whether MNT has MAX-independent functions. Using a MAX deficient cell line and siRNA-mediated silencing of MAX, we show that in the absence of MAX, the total MNT levels are elevated and that MNT localizes both in the cytoplasm and the nucleus. In contrast, MNT is predominantly nuclear when MAX is expressed. MNT is required for optimal cell proliferation even in the absence of MAX, being the first report of a MAX-independent function of MNT. Interestingly, MNT forms homodimers and autoregulates its expression by repressing its own promoter. The tight MNT regulation and its activity in absence of MAX suggest its importance on cell homeostasis.

INTRODUCTION

MNT (also called MXD6) is a basic helix-loop-helix leucine zipper (bHLHLZ) protein and it is the most divergent member of the MXD family, that also includes MXD1, MXI1, MXD3 and, MXD4. MNT forms heterodimers with MAX through the bHLHLZ domain, and binds to E-box DNA sequences. MYC is one of the most prevalent human oncoproteins. MYC can also interact with MAX and bind E-boxes *(Conacci-Sorrell et al 2014, Dang 2012)*. Whereas MYC-MAX, upon binding to E-boxes, acts primarily as transcriptional activator, the typical effect of MNT-MAX is the transcriptional repression *(Hurlin et al 1997, Meroni et al 1997)*. MNT can bind not only to MAX but also to the MAX-like HLH protein MLX *(Billin et al 1999, Meroni et al 2000)* which alternatively can interact with MLXIP (MONDOA) and MLXIPL (MONDOB) proteins. Therefore, MNT participates both in the MAX- and MLX-centred networks [reviewed in *(Diolaiti et al 2015, Yang & Hurlin 2017)*] serving as the link between the MAX-MYC and MLX-MONDO networks.

MNT is expressed constitutively in proliferating and quiescent cells and protein levels do not show major fluctuations when quiescent cells are mitotically stimulated *(Hurlin et al 1997 , Hurlin et al 2003, Walker et al 2005)* . MNT$^{-/-}$ mice are not viable *(Hurlin et al 2003, Toyo-oka et al 2004)* while MXD1$^{-/-}$, MXI1$^{-/-}$ and MXD3$^{-/-}$ mice survive, suggesting that MNT function is not redundant with that of the other MXD proteins *(Foley et al 1998, Queva et al 1999, Schreiber-Agus & DePinho 1998)*. Moreover, MNT is the only MXD protein in invertebrates *(Diolaiti et al 2015)*.

Consistent with MNT functioning as a MYC transcriptional antagonist, enforced MNT expression inhibits cell proliferation and impairs MYC-dependent transformation

63 *(Hurlin et al 1997, Walker et al 2005)*. The deficiency or down-regulation of MNT in
64 fibroblasts leads to increased proliferation (i.e., similarly to MYC-overexpression) and
65 partially rescues the proliferative arrest caused by MYC deficiency *(Dezfouli et al 2006,*
66 *Hurlin et al 2003, Nilsson et al 2004, Walker et al 2005)*. MNT ablation *in vivo* leads to
67 breast and T-cell tumors *(Dezfouli et al 2006, Hurlin et al 2003, Toyo-oka et al 2004)*,
68 and partial or total MNT deficiency in mice models impairs MYC-dependent
69 tumorigenesis *(Link et al 2012; Campbell et al 2017),* suggesting that *MNT* may function
70 as a tumor suppressor gene. On the other hand, *MNT* knock-out in some cell models
71 inhibits proliferation and promotes apoptosis *(Dezfouli et al 2006, Hurlin et al 2003,*
72 *Nilsson et al 2004)*. Thus, as MYC and MNT coexist in proliferating cells, it has been
73 suggested a role of MNT as a "buffer" of MYC activity.
74 In the present work we studied possible MAX-independent functions of MNT
75 using as the main model UR61 cells. These rat pheochromocytoma cells that do not
76 express a functional MAX protein but a truncated form (termed MAX^{PC12}) that lacks the
77 second helix and leucine zipper region of the bHLH-LZ domain which are the regions
78 responsible for dimerization with MYC and MNT *(Hopewell & Ziff 1995)*. Here we
79 describe a change of MNT subcellular localization depending on MAX expression and
80 that MNT is required for optimal cell proliferation even in the absence of MAX, being the
81 first example of a MAX-independent function of MNT. Finally, we show that MNT
82 transrepresses its own promoter and MNT ability to regulate gene expression in the
83 absence of MAX.
84
85
86 **RESULTS**

87 **MNT levels depend on MAX**

88 We first studied MNT levels in proliferating cells from eleven cell lines derived from
89 different tissues and species, including two cell lines lacking MAX: UR61 and human
90 small cell lung carcinoma H1417 cells *(Romero et al 2014)*. The results showed that,
91 although MNT expression varies among cell lines, the two MAX-deficient cell lines
92 expressed high MNT levels (*Figure 1A*). MNT was expressed in all cell lines as a protein
93 doublet, due to a slower migrating phosphorylated MNT form *(Popov et al 2005)*.
94 The high MNT expression in the two MAX-deficient cell lines led us to explore
95 whether MAX influenced MNT levels. For this purpose, we transfected UR61 cells with
96 a construct carrying human MAX cDNA driven by the metallothionein promoter, which is
97 activated by Zn^{2+} cations *(Canelles et al 1997)*. Several clones were isolated and two of

them with robust MAX induction were mixed and the resulting cell line was termed URMax34. We also generated a cell line transfected with the empty vector, termed URMT. The induction of MAX in response to Zn^{2+} in URMax34 cells was confirmed by

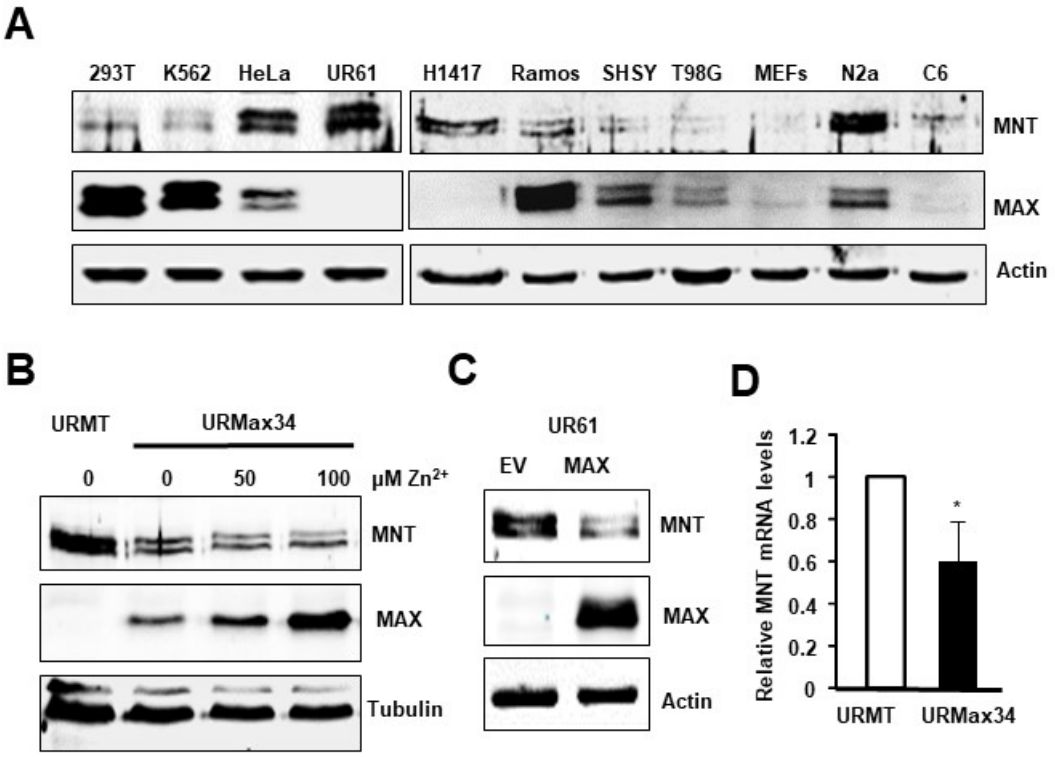

Figure 1. High MNT expression in MAX-deficient cells. (A) Cell lysates of the indicated cell lines were analyzed by immunoblot to determine the levels of MNT and MAX. β-actin levels were determined for protein loading control. The MAX-deficient cell lines analyzed were: UR61 (rat pheochromocytoma) and H1417 (human small cell lung carcinoma). The rest are MAX-expressing cells: HEK293T (human embryonic kidney, 293T), K562 (human chronic myeloid leukaemia), HeLa (human cervical cancer), Ramos (human B cell lymphoma), SH-SY-Y5 (SHSY, human neuroblastoma), T98G (human glioblastoma), MEFs (mouse embryonic fibroblasts), Neuro-2a (N2a, mouse neuroblastoma) and C6 (rat glioma). (B) Control URMT and URMax34 cells were treated for 24 h with 50 and 100 μM Zn^{+2} and the MNT and MAX protein expression were determined by immunoblot. α-tubulin levels were determined as a control for protein loading. The experiment was repeated three times. (C) Levels of MNT and MAX determined by immunoblot in UR61 cells 24 h after transfection with a MAX expression vector or the empty vector pCEFL (EV). β-actin levels are shown as a protein loading control. The result was reproduced in three experiments. (D) mRNA expression determined by RT-qPCR in URMT and URMax34 cells treated for 24 h with 100 μM Zn^{2+}. Data are represented as mean ±s.d. from three independent experiments, $^{*}P$ =0.012.

immunoblot (*Figure 1B*). We examined the effect of MAX induction on MNT levels in URMax34 cells. The results showed that MNT was down-regulated upon MAX induction by Zn^{2+} (*Figure 1B*). To confirm this result and rule out effects potentially related to the generation of stably transfected clones (as URMax34 system), UR61 cells were transiently transfected with a MAX expression vector and the results showed a decrease in MNT protein levels in MAX-transfected cells (*Figure 1C*). It is noteworthy that the r-expression of MAX in these cells provoked the down-regulation of MNT at the mRNA levels, as determined by RT-qPCR (*Figure 1D*).

109 We sought to confirm this in a different cell type and species. For this purpose, a
110 MAX expression vector was transfected into human myeloid leukemia K562 cells. The
111 immunoblot results showed lower MNT levels in the cells with MAX overexpression
112 (*Figure 2A*). Next, we used the Kmax12 cell line *(Canelles et al 1997)*, a K562 derivative
113 carrying a MAX transgene which expression is induced by Zn^{2+}. Induction of MAX

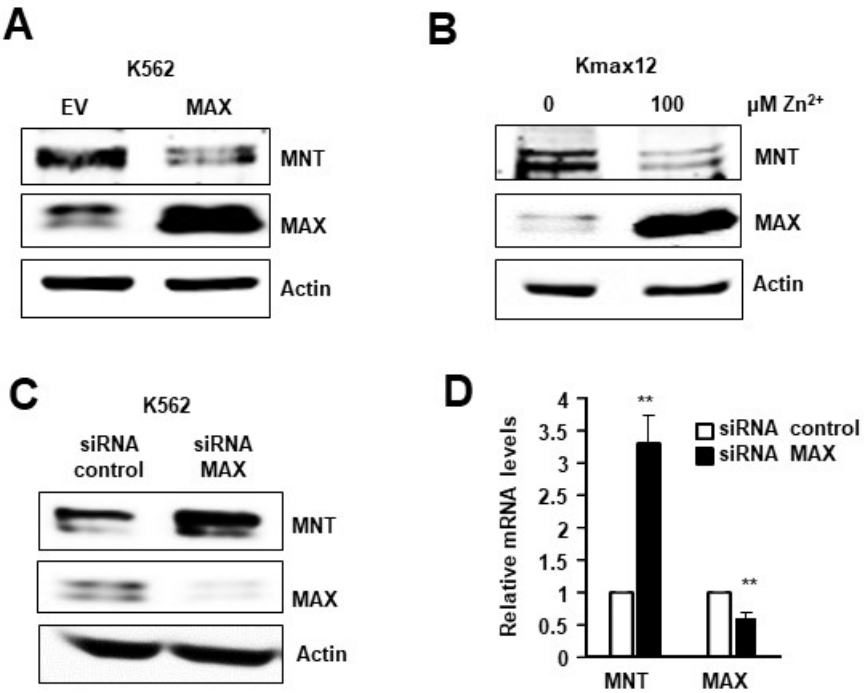

Figure 2. MAX regulates MNT expression in K562 cells. (A) MNT and MAX levels determined by immunoblot in K562 cells 24 h after transfection with a MAX expression vector. The results were reproduced in three biological replicates (B) MNT and MAX levels determined by immunoblot in Kmax12 cells treated for 48 h with 100 μM Zn^{2+} to induce MAX expression. The results were reproduced in three biological replicatess. (C) MNT and MAX protein expression analyzed by immunoblot in K562 48 h after transfection with siRNA against *MAX* gene. β-actin levels are shown as a protein loading control. The results were reproduced in two experiments. (D) MNT and MAX mRNA expression analyzed by RT-qPCR 48 h after transfection with siRNA against *MAX* gene. Data are shown as mean ± s.d. of three biological replicates. *P <0.005

114 expression in Kmax12 cells resulted in a concomitant MNT downregulation (*Figure 2B*).
115 We also used the opposite approach, i.e. depleting cells of MAX and analyzing the
116 expression of MNT. As shown in *Figure 2C*, MNT protein expression was upregulated
117 when MAX was silenced with siRNA in K562. Interestingly, MNT mRNA was also up-
118 regulated in MAX-silenced cells (*Figure 2D*). Altogether, the results showed that low MAX
119 levels result in MNT up-regulation, likely at the transcriptional level.
120

121 **MNT binds and repress its own promoter in the presence of MAX**

122 The above results showing that MNT down-regulation took place at the mRNA
123 level prompted us to investigate if MNT impairs the activity of its own promoter.

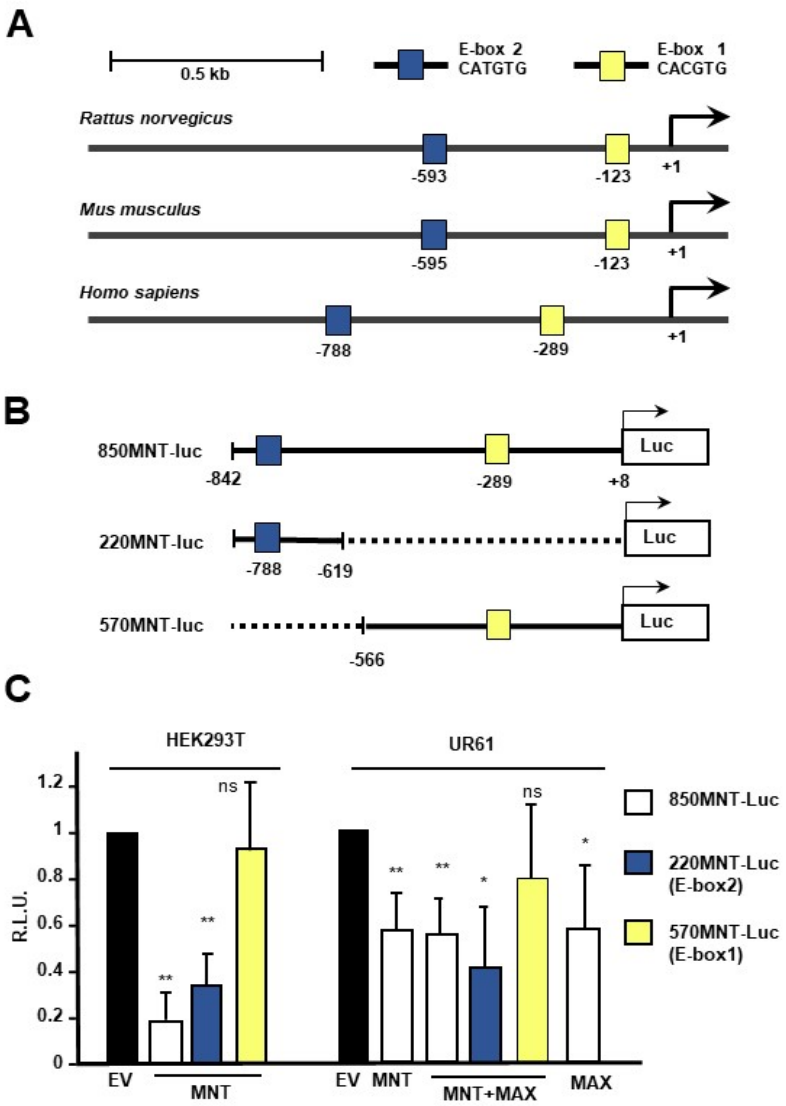

Figure 3. MNT regulates its own promoter. (A) Schematic representation of human, rat and mouse MNT promoters showing two conserved E-boxes. The coordinates correspond to the 5' nucleotide of each E-box, using the UCSC genome browser (http://genome.ucsc.edu/, release GRCh37/hg19). (B) Schematic representation of luciferase reporters driven by human MNT promoter generated in this work. The longest reporter (850 bp upstream the transcription start site) contains two conserved E-boxes. The coordinates are as in USCS browser (release GRCh37/hg19). (C) Luciferase assays in the indicated cell lines transfected with the reporters described above plus MNT and/or MAX expressing vectors or the corresponding empty vectors (EV). Luciferase activity was assayed 36 h or 24 h after transfection of UR61 and HEK293T cells, respectively. The data are shown as mean ± s.e.m. of 9 (for 850MNT-luc) or 4 independent transfections (for the rest of experimental points). $^{**}P < 0.005$; $^{*}P < 0.01$.

Bioinformatic analysis of human, mouse and rat MNT promoter regions revealed that there are two E-box sequences within 1 kb upstream the transcriptional start site of *MNT* (one canonical E-box, CACGTG (E-box 1), and one non-canonical, CATGTG (E-box 2) that are conserved among these three different species (*Figure 3A*).

We then constructed a luciferase reporter carrying the 850 bp upstream region of the transcription start site from the human MNT gene. The construct was termed 850MNT-Luc (*Figure 3B*). HEK293T cells (which express MAX) were transfected with the 850MNT-Luc and MNT expression vectors. The results showed that MNT overexpression led to a reduction in the luciferase activity (*Figure 3C*), suggesting that

133 MNT-MAX negatively regulates the MNT promoter. To determine the contribution of the
134 two E-boxes in the MNT-mediated negative autoregulation we constructed two reporters
135 containing each of the E-boxes, termed 220MNT-Luc (containing the last 220 bp of the
136 850MNT-Luc reporter which includes the E-box 2) and 570MNT-Luc (containing the first
137 570 bp of the 850MNT-Luc reporter which includes the E-box 1) (*Figure 3B*). The
138 luciferase assays in HEK293T cells showed that the E-box 2, mapping at –788 was
139 critical for MNT-mediated downregulation of its own promoter (*Figure 3C*, left panel).

140 We also investigated the activity of the MNT promoter in UR61 cells, which do
141 not express MAX. UR61 cells were transfected with the 850MNT-Luc vector together
142 with MNT and MAX expression vectors. The results also showed a decrease in the
143 luciferase activity although less than in HEK293T cells (*Figure 3C*, right panel). The
144 expression of MNT alone also led to a decrease in the luciferase activity, suggesting that
145 MNT can downregulate MNT promoter in UR61 cells in the absence of MAX. The
146 repressive effect of MNT was stronger in HEK293T cells than in UR61 cells, which may
147 be explained by the limited
148 overexpression of MNT protein achieved
149 in transfected UR61 cells (shown
150 below). Co-transfection of MNT and
151 MAX resulted in a decrease in the
152 activity of both promoter constructs
153 (850MNT-Luc and 220MNT-Luc,
154 carrying fragments of the human MNT
155 promoter of 842 and 223 bp,
156 respectively). Since MNT-MAX dimers
157 bind E-boxes in the promoters to repress
158 transcription, we analysed the ChIP-seq
159 data published by the ENCODE project
160 (http://genome.ucsc.edu/ENCODE).
161 The data revealed two regions bound by
162 MAX in the human *MNT* promoter that
163 encompass the two E-boxes (*Figure*
164 *4A*). We also analysed the ChIP peaks
165 for MAX, MYC and MXI1 proteins on the
166 *MNT* promoter in other human cell lines
167 as H1ES, HeLa, NB4, A549, GM78,
168 HEPG, SKSM and IMR90. The analysis
169 revealed that the three proteins

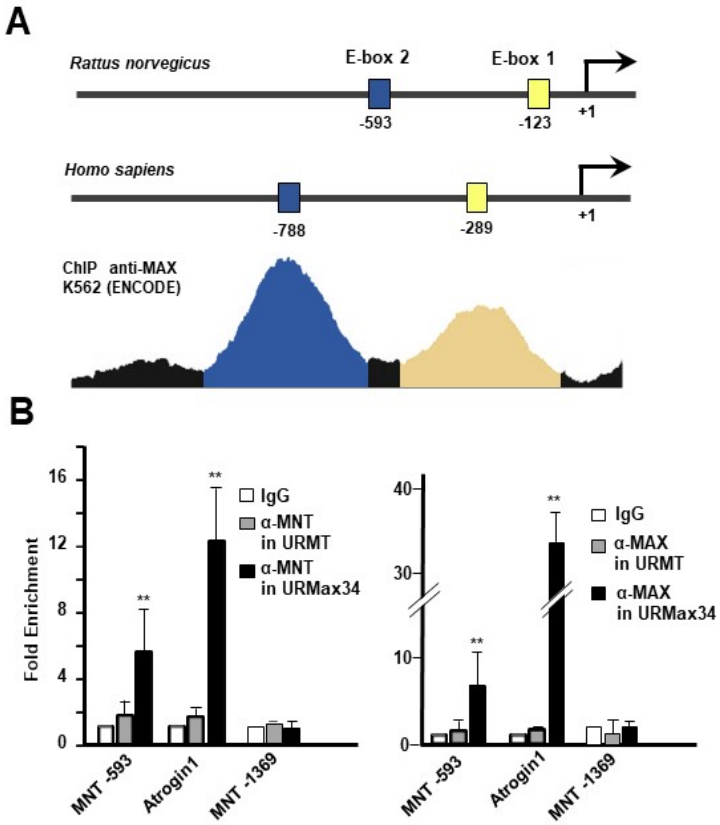

Figure 4. MNT binds to *MNT* promoter. (A) Schematic representation of human and rat MNT promoters showing the peaks for MAX of the ChIP experiments with anti-MAX antibody on human K562 cell line as published by the ENCODE project. (B) ChIP with anti-MNT (left) and anti-MAX (right) antibodies on the MNT promoter of URMT and URMax34 cells, both treated with 100 μM Zn^{2+} for 24 h. MNT and MAX binding to *MNT* gene promoter in the region containing the E-box 2 (-593 in rat gene) was studied by qPCR. Amplicons from Atrogin-1 (*FBX032*) were used as positive control for MNT binding and a region 1389 bp upstream from the TSS without E-boxes was used as negative control. The data are means ±s.e.m. from four independent experiments. * $P<0.05$.

170 presented peaks at the same positions near the transcription start site of the human MNT
171 gene (*Figure 4-figure supplement 1*), suggesting that members of the MYC and MXD
172 family bind and possibly regulate the promoter of *MNT*.

173 As MNT was downregulated when MAX was re-expressed, we hypothesized that
174 MNT-MAX heterodimers might bind to the *MNT* promoter and down-regulate its own
175 expression. To explore this hypothesis,
176 a ChIP assay was performed with MNT
177 and MAX antibodies in URMT and
178 URMax34 treated with Zn^{2+} to induce
179 MAX. We studied the -593 E-box of the
180 *MNT* promoter, as well as a region of the
181 *Atrogin-1 (FBXO32)* promoter as a
182 positive control for MNT binding
183 *(Terragni et al 2011)*. A region mapping
184 at 1369 bp upstream on MNT
185 transcription start site with no E-boxes
186 was used as negative control. As shown
187 in *Figure 4B*, MNT and MAX bound to
188 the *MNT* promoter in URMax34 cells.
189 However, in the MAX-deficient control
190 URMT cells, neither MNT nor MAX were
191 bound to the *MNT* promoter. In the same
192 way, MNT and MAX were bound to the
193 positive control *Atrogin-1* promoter in
194 URMax34 but not in URMT control cells
195 (*Figure 4B*). These data show that MNT
196 most likely binds to its own promoter as
197 a heterodimer with MAX and suggest a
198 possible negative regulation of MNT own
199 expression.

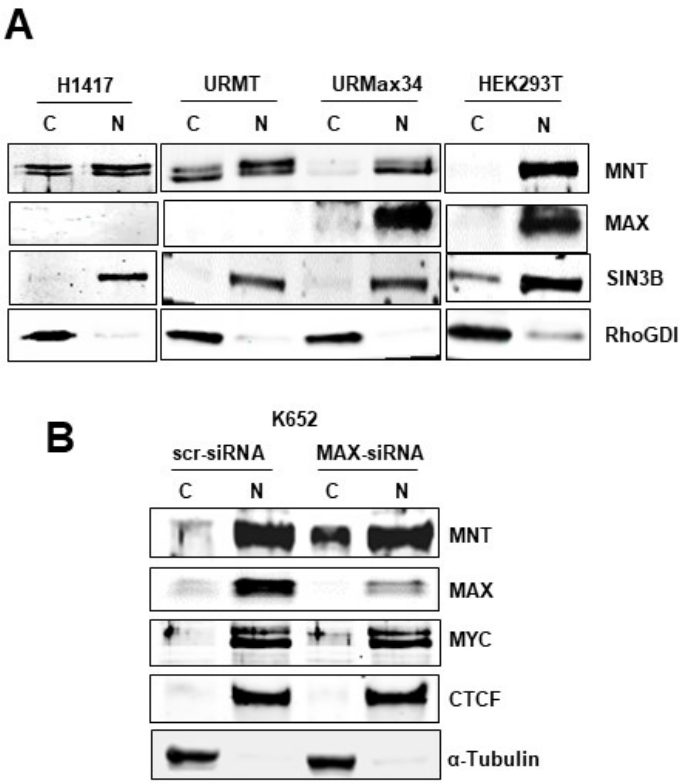

Figure 5. MNT subcellular localization depends on MAX. (A) Cell extracts were subjected to cytoplasmic/nuclear fractionation in H1417 (human lung cells deficient in MAX), HEK293T, URMT and URMax34 treated for 24 h with 100 μM Zn^{2+} to induce MAX. The levels of MNT and MAX were determined in each fraction by immunoblot. SIN3B and RhoGDI (ARHGDIA) were used as nuclear and cytoplasmic markers respectively. "C" refers to cytoplasmic fraction and "N" to nuclear fraction. Similar results were obtained in three biological replicates. (B) K562 were transfected with siRNA against the *MAX* gene and 48 h later cell extracts were prepared and subjected to cytoplasmic/nuclear fractionation. The expression of MAX, MNT and MYC were analyzed by immunoblot. The expression of CTCF and α-tubulin were analyzed as a control for nuclear and cytoplasmic proteins respectively. scrRNA, control scrambled siRNA. The results were reproduced in three biological replicates.

200

201 **MNT localizes in the cytoplasm of MAX-deficient cells**

202 We next examined the subcellular localization of the excess MNT present in MAX-
203 deficient cells. URMT and URMax34 cells were treated with Zn^{2+} to induce MAX and we
204 performed a cytoplasmic and nuclear fractionation to analyse MNT levels. In control
205 URMT cells, MNT protein was found in the nuclear fraction, as expected, but also at
206 similar levels in the cytoplasm. In contrast, in URMax34 expressing MAX, MNT protein

207 was found only in the nucleus (*Figure 5A*), the localization typically found for MNT *(Lafita-*
208 *Navarro et al 2016)*. We were not able to use untreated URMax34 cells as a control as
209 they express some MAX even in the absence of Zn^{2+} (*Figure 1B*). Cytoplasmic MNT
210 was also observed in H1417 cells, human cells deficient in MAX. As a control, the
211 localization of MNT was analysed in HEK293T cells, that express the MAX protein.
212 Cytoplasm/nucleus fractionation revealed that MNT and MAX were localised in the
213 nucleus but not in the cytoplasm of HEK293T cells (*Figure 5A*). To test if the localization
214 of MNT depended on MAX, we silenced the MAX protein in K562 cells with siRNA and
215 we carried out cytoplasm/nucleus fractionation. In control K562 cells, MNT and MAX
216 were mainly localised in the nucleus. In contrast, in MAX-depleted cells, a significant
217 amount of MNT was found in the cytoplasm of K562 cells (*Figure 5B*). It is noteworthy
218 that nuclear MNT levels were similar in URMT and URMax34, as well as in control K562
219 and MAX-depleted K562 cells. As controls for nuclear proteins, we used MYC and CTCF
220 (*Figure 5B*). Taken together, the data indicates that MAX absence leads to an
221 upregulation of MNT protein and that the excess of MNT accumulates in the cytoplasm.
222

223 **MNT knock-down impairs cell proliferation in MAX-deficient cells**

224 We next asked for a possible biological effect of MNT on cell proliferation in the UR61
225 MAX-deficient cells. We decided to knock-down MNT through siRNAs. For this, we used
226 lentiviral particles containing two short-hairpin constructs against the rat MNT gene. Two
227 shMNT constructs that efficiently reduced MNT levels were used, termed shMNT-1 and
228 shMNT-2 (*Figure 6A*). The vectors also carried a puromycin-resistance gene. UR61 cells
229 were transiently co-transfected with the shMNT constructs (or the empty vector) and a
230 GFP expression vector in a proportion 1:5 to ensure that the GFP-positive cells also
231 incorporated the shMNT plasmid. Six days after transfection, the fraction of GFP positive
232 cells were analysed by flow cytometry. The results showed that the fraction of GFP
233 positive cells was clearly reduced in cells with depleted MNT (*Figure 6B*), suggesting
234 that MNT loss resulted in impaired cell proliferation. In a second approach, we
235 transfected the UR61 cells with the sh-MNT constructs and counted viable cells after 3
236 and 7 days of transfection. As shown in *Figure 6C,* MNT-silenced UR61 cells grew slower
237 than controls. We also performed clonogenic assays in UR61 transfected with the
238 shMNT and/or a MAX expression vector (in 1:3 proportions to ensure that the shMNT
239 containing cells had also incorporated the MAX vector) as well as the empty vectors. 24
240 h after transfection puromycin was added and after selection the colonies were stained
241 with crystal violet, the dye was solubilised and quantified. The results showed that MNT
242 depletion provoked a dramatic growth inhibition. These results of MNT depletion

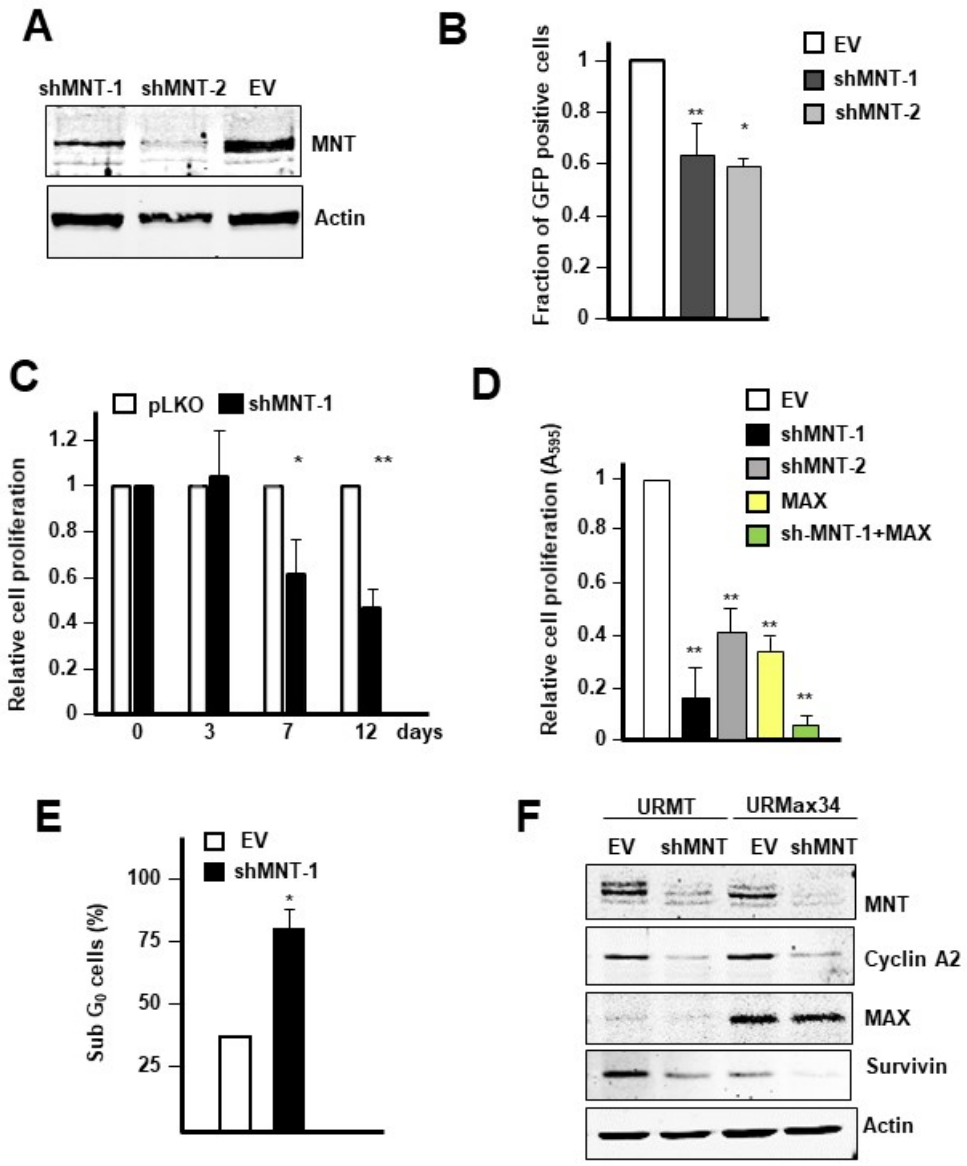

Figure 6. MNT knock-down impairs cell proliferation in MAX-deficient cells. (A) Silencing of MNT by short-hairpin constructs. URMT cells were transfected with vectors encoding sh-MNT-1 and shMNT-2. 24 h after transfection the cells were treated with puromycin (0,3 µg/ml) and 72 h after transfection the cells were lysed and the levels of MNT analyzed by immunoblot. β-actin levels were determined as a control for protein loading. (B) Fraction of GFP-expressing UR61 cells assessed by flow cytometry 7 days after co-transfection with GFP and shMNT vectors (in proportion 1:5) and analyzed by flow cytometry. The data are shown as mean ± s.e.m. of three independent experiments, **P* =0.006, ***P* =0.008. (C) Cell proliferation determined by cell counting at 3, 7 and 12 days after transfection of shMNT-1 or the empty vector pLKO1. The data are shown as relative mean values ± s.e.m. of three independent experiments, **P* = 0.01, ***P* = 0.008 (D) Cell growth determined by crystal violet staining in UR61 cells transfected with the indicated vectors. After 15 days of puromycin selection the colonies were stained with crystal violet and the dye was solubilised and quantified by absorbance at 595 nm. EV, empty vector (pLKO for shMNTs and pCEFL for MAX). **P < 0.005. Data show mean values ± s.d. from three independent experiments. (E) Fraction of sub G_0 UR61 cells transfected with the shMNT-1 vector and empty vector (EV). Cells were fixed and stained with propidium iodide at day 6 post-transfection and puromycin selection. The percentage of cells containing less than 2C DNA content was determined by flow cytometry. The data are mean values of three independent experiments ± s.d., **P* =0.014. (F) Levels of MNT determined by immunoblot in URMT and URMax34 cells 72 h after transfection with the shMNT vector and treated for 12 h with 100 µM Zn^{2+}. MAX, cyclin A2 and survivin (BIRC5) were also determined. β-actin levels were determined for protein loading control. Two experiments were performed with similar results.

impairing cellular proliferation in a MAX-independent manner are unprecedented. These results also showed that UR61 cells overexpressing the MAX protein grew more slowly

246 than the control *(Figure 6D),* confirming the effect previously reported for the MAX-
247 deficient PC12 pheochromocytoma cells (UR61 parental cells) *(Hopewell & Ziff 1995)*.
248 In addition, when MNT silencing was accompanied by MAX enforced expression, the
249 inhibition of UR61 cell proliferation was stronger (*Figure 6D*). Consistent with the anti-
250 proliferative effects of MNT depletion, we failed to generate stable MNT-silenced UR61
251 cell lines (not shown). In order to generate UR61 cells with MNT overexpression we
252 transfected UR61 with MNT expression vectors but we were not able to detect a
253 significant increase in MNT protein levels upon transfection. This is likely due to the
254 autoregulation of MNT protein levels, as the overexpression of MNT protein was readily
255 detected by immunoblot when the transfected cells were treated with the proteasome
256 inhibitor bortezomib (*Figure 6-figure supplement 1A*). In contrast, some increase in the
257 levels of MNT was detected when MNT was transfected in MAX-expressing URMax34
258 cells (*Figure 6-figure supplement 1B)* or when MNT was co-transfected with MAX in
259 UR61 cells (*Figure 6-figure supplement 1C*).
260 Since the depletion of MNT impairs cell proliferation of UR61 cells, we wondered
261 whether this was accompanied by cell death. To study this, the levels of survivin (BIRC5)
262 in URMT and URMax34 were analysed by immunoblot (*Figure 6F*) and the results
263 showed a decrease in survivin and cyclin A (a marker of proliferation) in cells with
264 depleted MNT, both in MAX-deficient cells (compare lanes 1 vs 2 in *Figure 6F*) and in
265 MAX-expressing cells (compare lanes 3 vs 4 in *Figure 6F*), although the effect was
266 stronger in these latter cells. To check the contribution of apoptosis, we also measured
267 DNA content flow cytometry. We found that the fraction of cells with a sub-G0 amount of
268 DNA was higher in cells transfected with the shMNT vector (*Figure 6E*). The results
269 suggest that the depletion of MNT leads to cell proliferation arrest and apoptosis in UR61.

270 MNT modifies gene expression in MAX-deficient cells

271 Since the data shown above indicated that MNT knock-down in UR61 cells leads to
272 growth arrest and cell death, and considering that MNT is a transcription factor, we set
273 out to study if MNT regulates the transcriptional program in the absence of MAX. For this
274 purpose, we investigated the effects of MNT depletion on the transcriptome of cells with
275 and without MAX. URMT and URMax34 cells were transfected with the short-hairpin
276 RNA construct against the rat MNT gene (shMNT-1) or the empty vector as control in
277 two different biological replicates. We first checked the appropriate conditions to
278 efficiently silence the expression of MNT upon transfection of the shMNT constructs in
279 URMT and URMax34 cells. A significant MNT depletion was consistently achieved at 72
280 h post-transfection (not shown). Thus, for the RNAseq experiment, the URMT and

281 URMax34 cells were transfected with the shMNT-1 construct and two days after
282 transfection, cells were treated with Zn^{2+} for 24 h to achieve significant MAX-induced
283 expression (in URMax34) as well as significant MNT depletion (*Figure 7A*). Two

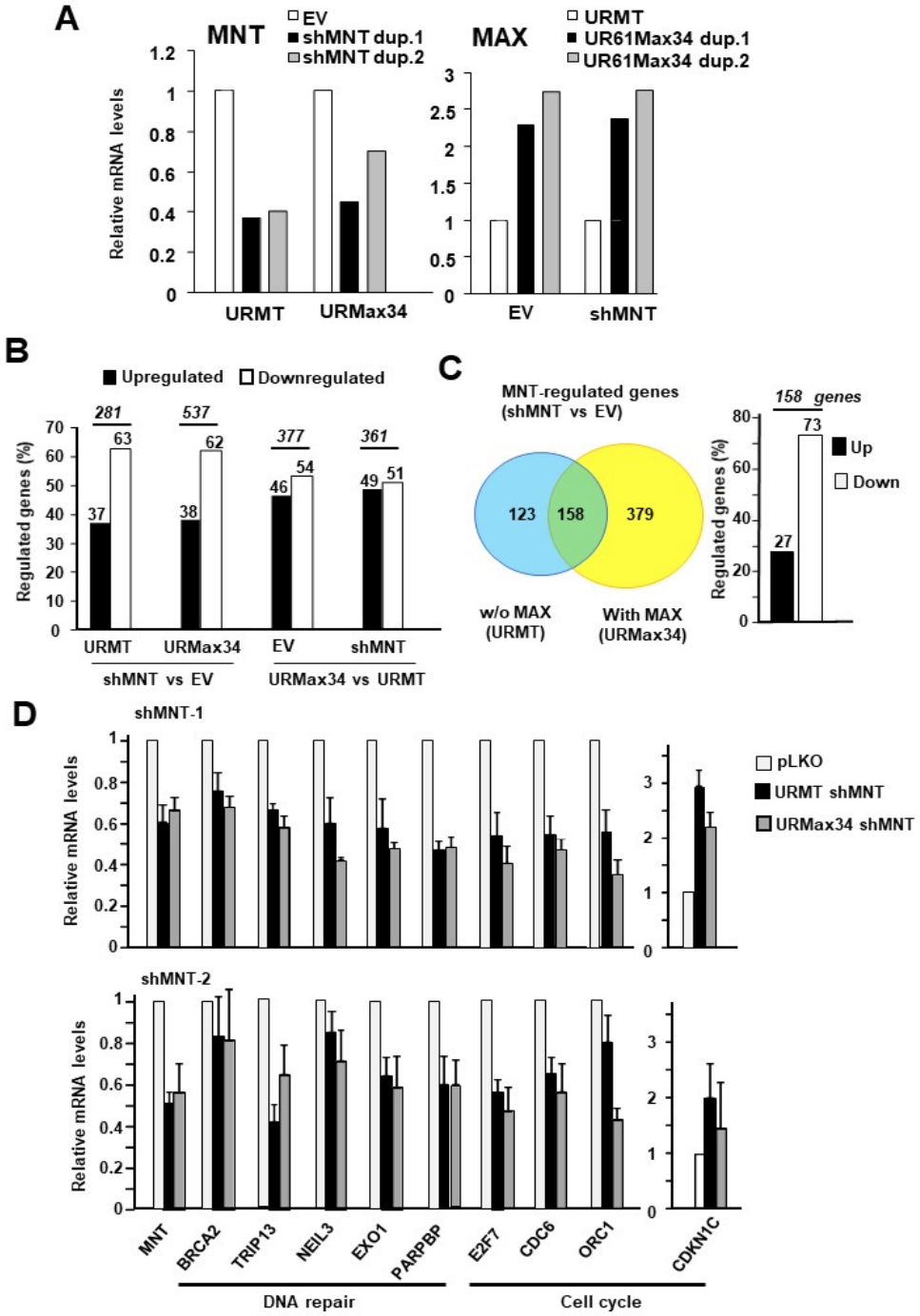

Figure 7. Gene expression changes in MNT knock-down cells. (A) mRNA expression of MNT and MAX in URMT and URMax34 cells lysed 72 h after transfection with shMNT and 24 h of treatment with 100 µM Zn^{2+}. The experiments were performed in duplicated (dup.1 and dup.2) biological replicates. These RNAs were subjected to RNA-seq. (B) Percentage of upregulated and downregulated genes in cells transfected with the shMNT or pLKO (empty) vectors in URMT and URMax34 cells, as indicated at the bottom. The number of genes regulated comparing the different samples are indicated at the top of the figure. The gene inclusion criteria were a change in mRNA level ≥0.7 or ≤-0.7 log2 FPKM fold change. The RNA-seq data are from two independent experiments. The genes regulated in the different comparisons are listed in the *Supplementary Files 1 to 4*. (C) Venn diagram showing the genes that are regulated by MNT in MAX-deficient (URMT) or MAX-expressing cells (URMax34). The graph at the right shows the number of up- or down-regulated genes in the group of overlapping genes. (D) mRNA expression regulation due to MNT silencing in genes selected after the RNA-seq data analysis. URMT and URMax34 were transfected with shMNT-1 (upper panel) and shMNT-2 (lower panel) or empty vector pLKO. After 48 h cells were treated for 24 h with 100 µM Zn^{2+}, total RNA was prepared and mRNA levels of the indicated genes were determined by RT-qPCR . Most of the selected genes are involved in DNA repair or cell cycle as indicated at the bottom. The data are represented as mean ±s.e.m. from four (shMNT-1) or three (shMNT-2) independent transfection experiments. In all cases, P <0.05..

284 independent transfections and RNA preparations of each cell line were submitted for
285 next generation sequencing RNA-seq and the data was processed bioinformatically as
286 escribed in the Methods section.

287 Once we obtained the expression values of each experimental replicate we
288 compared the different conditions. For all of the different comparison we grouped the
289 genes that were up-regulated and down-regulated in both biological replicates
290 considering a log2 RPKM fold change higher than 0.7 or smaller than -0.7 of the
291 corresponding control and a p-value < 0.1. The heatmaps of the gene expression
292 signatures clearly showed that the depletion of MNT in both URMT and URMax34
293 induced gene expression changes (*Figure 7-figure supplement 1*) indicating that MNT
294 can be involved in transcriptional regulation without the concourse of MAX. Specifically,
295 281 genes were regulated upon MNT depletion in MAX-deficient URMT cells (*Figure 7-*
296 *figure supplement 2*) and 537 genes in MAX-expressing cells (i.e., URMax34 treated with
297 Zn^{2+}) (*Figure 7-figure supplement 3*). Of those, approximately 62 % of the genes were
298 down-regulated upon MNT depletion in both cell lines (*Figure 7B*). In addition, the
299 URMax34 vs URMT gene expression signatures heatmaps also showed that the
300 expression of MAX induced gene transcriptional changes independently of MNT
301 depletion (*Figure 7-figure supplement 1*). Specifically, 377 genes were found to be
302 differentially expressed when comparing URMax34 and URMT cells (*Figure 7-figure*
303 *supplement 4*) and 361 genes when comparing URMax34 and URMT cells depleted of
304 MNT (*Figure 7-figure supplement 5*). Among *MAX*-regulated genes, roughly half of the
305 genes were downregulated (*Figure 7B*). Importantly, the comparison between the lists of
306 differentially expressed genes upon MNT-depletion in cells without MAX (URMT) and
307 with MAX (URMax34) revealed 158 shared genes in the two biological replicates (*Figure*
308 *7-figure supplement 6)*. This indicated that 56% and 30% of MNT-induced transcriptional
309 changes in each cell line respectively are regulated by MNT in a MAX-independent
310 manner (*Figure 7C*).

311 The genes showing expression changes in the MNT-depleted URMT and
312 URMax34 cells were analyzed with the GSEA and the MsigDB platform
313 (http://software.broadinstitute.org/gsea/msigdb). The genes regulated upon MNT knock-
314 down were compared with the gene sets derived from the biological process gene
315 ontology and the comparison showed that genes belonging to cell cycle processes are
316 the most enriched set in MNT-depleted cells both in MAX expressing and not expressing
317 cells (*Figure 7-figure supplement 7)*. This functional analysis of the gene transcriptional
318 signatures are consistent with the biological effects of MNT-depletion in cell proliferation.

319 Thus, in order to explain and confirm the effects of MNT ablation on UR61 cell
320 growth, we selected several genes involved in cell cycle and DNA replication which

321 expression was changed according to the RNA-seq analysis. URMT and URMax34 cells
322 were transfected with the two shMNT constructs and the empty vector following the same
323 conditions as the conditions used for the RNAseq experiment. The expression of the
324 selected genes was analyzed by RT-qPCR. *Figure 7D* shows that genes involved in cell

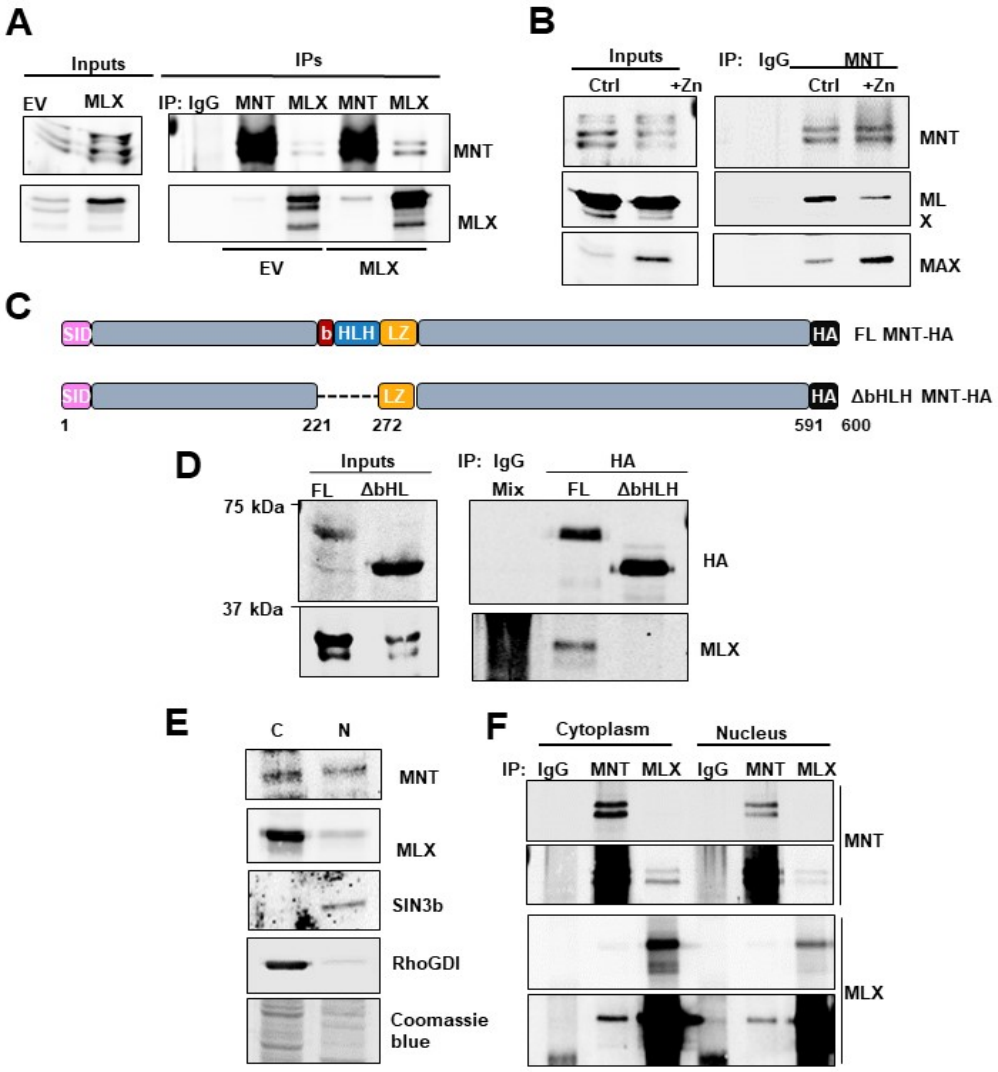

Figure 8. MNT and MLX interaction in UR61 cells. (A) URMT cells were transfected with a MLX expression vector or the empty vector (EV). 48 h after transfection, total cell lysates were prepared and precipitated with anti-MNT or anti-MLX antibodies, as well as unspecific IgG. The presence of MNT and MLX were detected in the immunoprecipitates by immunoblot. The results were reproduced in two experiments (B) URMax34 cells were transfected with a MLX expression vector and 48 h after transfection cells were treated with 100 µM Zn^{2+} for 24 h. Then total cell lysates were prepared and immunoprecipitated with anti-MNT. As a control, a mixture of lysates from cells treated and untreated with Zn^{2+} was immunoprecipitated with unspecific IgG. The presence of MNT, MLX and MAX in the immunoprecipitates were analysed by immunoblot. The results were reproduced in three experiments immunoprecipitations. (C) Schematic representation of the full-length (FL) and the deletion mutant ΔHLH MNT-HA used in subsequent experiments. The SID (Sin3 Interacting Domain), bHLH, LZ domains, HA tag and amino acids of the murine protein are indicated. (D) URMT cells were co-transfected with a vector expressing MLX and the constructs shown in (C) as indicated at the top. 48 h after transfection, cell lysates were prepared and the cells were immunoprecipitated with mouse anti-HA antibody to pull down the exogenous MNT proteins constructs. As a control, lysates (a mixture of lysates from cell transfected with FL MNT and ΔHLH MNT) were also immunoprecipitated with unspecific IgGs. The immunoblot analysis using a rat monoclonal anti-HA antibody revealed the presence of FL MNT and the smaller ΔHLH MNT The presence of MLX in the immunoprecipitates was analysed with an anti-MLX antibody. (E) MLX localization in UR61 cells. Nuclear ("N") and cytoplasmic ("C") extracts were prepared from URMT cells as described in Materials and Methods and the levels of MNT and MLX were determined in each fraction by immunoblot. SIN3B and RhoGDI (ARHGDIA) were used as nuclear and cytoplasmic markers respectively. The antibodies used are as described in the *Supplementary File 1*. A picture of the gel stained with Coomasie Blue after transference is also shown as an indicator of the total amount of proteins in the cytoplasmic and nuclear fraction. (F) Interaction between MNT and MLX in the nucleus and cytoplasm. URMT cells were transfected with a MLX expression vector and 48 h later nuclear and cytoplasmic extracts were prepared and immunoprecipitated with anti-MNT or anti-MLX antibodies. The levels of MNT and MLX in the immunoprecipitates were assayed by immunoblot. The results were reproduce in two independent experiments

325 cycle and DNA replication (*E2F7*, *CDKN1C*, *CDC6*, *ORC1*) and, DNA repair (*BRCA2*,
326 *TRIP13*, *NEIL3*, *EXO1*, *PARPB*), were down-regulated upon silencing of *MNT* with the
327 two shMNT constructs, except *CDKN1C* (p57, a cell cycle inhibitor) which was up-
328 regulated. Altogether, the results are consistent with the negative effect of MNT depletion
329 on cell proliferation in UR61 cells (*Figure 6*).

330 We then wondered how could MNT act as a transcription factor in cells lacking
331 MAX. Besides MAX, MNT can also bind the HLH protein MLX *(Cairo et al 2001, Meroni*
332 *et al 2000)*. To show if this interaction also takes place in UR61, we transfected MLX-
333 Flag into URMT cells and 48 h later lysates were immunoprecipitated with anti-MLX
334 antibody and anti-MNT antibodies. The immunoprecipitates were analysed by
335 immunoblot and the results showed the interaction between MNT and MLX (*Figure 8A*).
336 We next studied this interaction in URMax34 cells treated with Zn^{2+}, i.e. cells expressing
337 MAX. The immunoblot results showed that MNT and MLX also interacted but the
338 interaction was weaker when MAX expression was induced by Zn^{2+}. Thus, the data
339 suggest that, at least in our experimental conditions, MNT-MAX dimers were formed
340 more efficiently than MNT-MLX dimers (*Figure 8B*). To confirm the MNT-MLX interaction
341 in URMT cells, we prepared a HA-tagged MNT mutant with a deletion of most of the HLH
342 domain of mouse MNT, termed ΔHLHMNT-HA (*Figure 8C*). This mutant or the wild-type
343 counterpart was transfected into URMT and the corresponding lysates were
344 immunoprecipitated with anti-HA. The results showed that HLH domain is required for
345 the MNT-MLX interaction (*Figure 8D*).

346 In contrast to MAX, MLX is expressed in both nucleus and cytoplasm *(Billin et al*
347 *2000)*. By immunoblot analysis it was found that MLX was present in nucleus and, at a
348 lesser extent, in the cytoplasm of URMT cells (*Figure 8E*). Next, we prepared nuclear
349 and cytoplasmic fractions of URMT cells and studied by immunoprecipitation with anti-
350 MNT and anti-MLX antibodies if MNT and MLX interact. The results showed that this was
351 indeed the case in both nuclear and cytoplasmic fractions (*Figure 8F*). The proximity
352 ligation assay also showed that MNT and MLX interacted in both nucleus and cytoplasm
353 (not shown).

354 Finally, it is described that MNT can form homodimers in two-hybrid experiments
355 *(Hurlin et al 1997, Meroni et al 1997)*. Thus, a possibility is that MNT acts a transcription
356 factor as a homodimer. This homodimerization has not been demonstrated *in vivo* so we
357 tested it in HEK293T and UR61 cells. We first co-transfected HEK293T cells with GFP-
358 MNT and Flag-MNT constructs and immunoprecipitated with anti-GFP antibody. The
359 immunoblot analysis demonstrated the presence of the smaller Flag-MNT protein in the
360 material immunoprecipitated with anti-GFP (*Figure 9A*). As expected, both big and small
361 MNT forms were detected when the immunoblots were analysed with anti-MNT antibody

362 (*Figure 9A*). The results suggested the presence of homodimers between GFP-MNT and
363 MNT-Flag in HEK293T cells. As a control, the lysates with anti-MAX antibody were
364 imunoprecipitated, and both MNT and GFP-MNT were found to be bound to MAX (not
365 shown). Next, we investigated the MNT homodimerization in the UR61 system. URMT

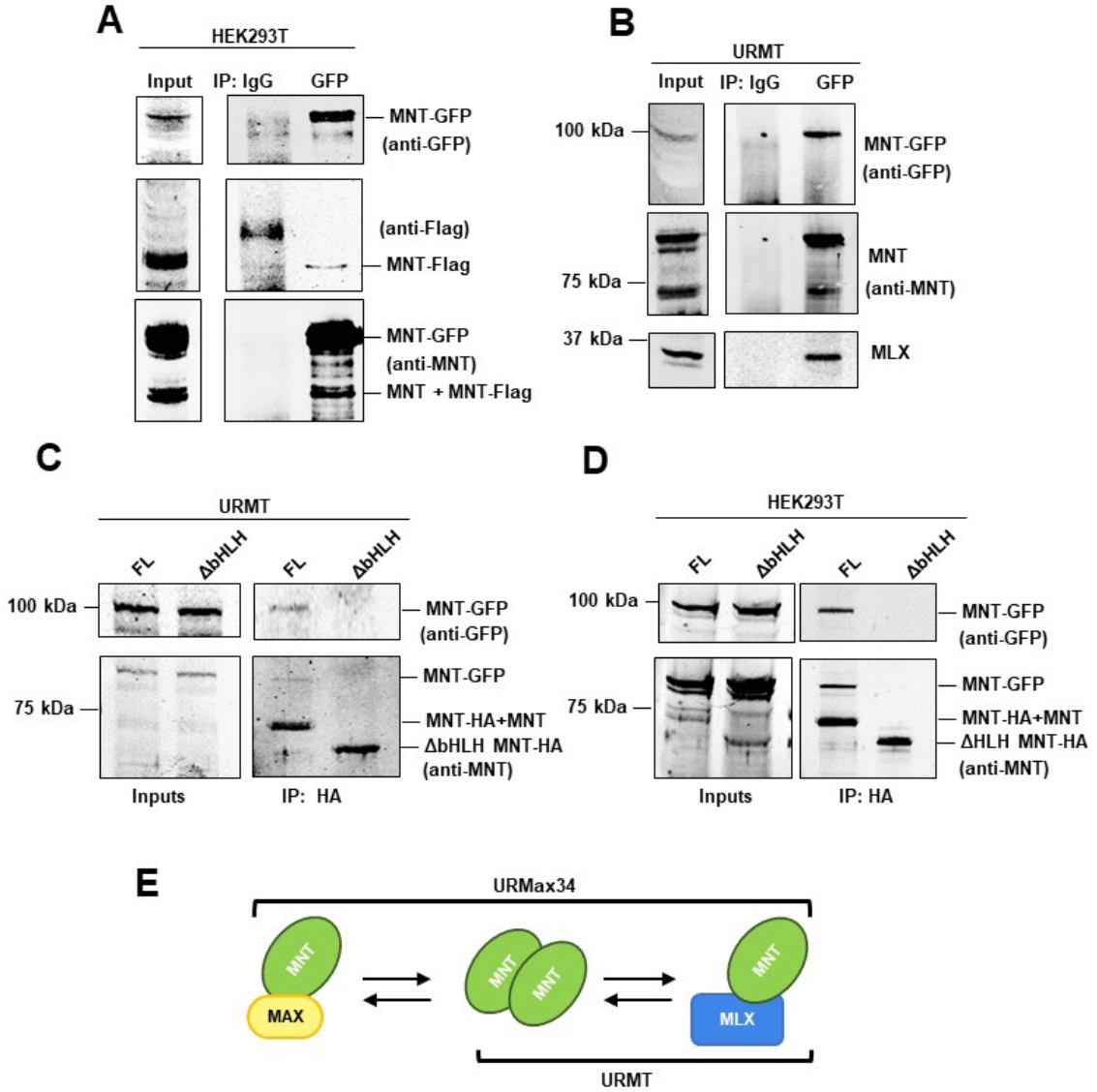

Figure 9. MNT homodimerization in UR61 cells. (A) HEK293T cells were co-transfected with a GFP-MNT and MNT-Flag expression vectors, and 24 h later lysates were prepared and immunoprecipitated with anti-GFP antibody. The presence of MNT-GFP and MNT-Flag were revealed by immunoblotting the antibodies indicated at the right. As a control, lysates were precipitated with unspecific IgG. The antibodies used in each immunoblot are indicated at the right. The results were reproduced in two immunoprecipitations. (B) URMT cells were infected with lentivirus encoding a MNT-GFP and 72 h later were transfected with MNT-Flag and treated with 15 nM bortezomib for 12 h before harvesting. 48 h after transfection lysates were prepared and immunoprecipitated with anti-GFP antibody. The presence of MNT-GFP, MNT and MLX in the immunoprecipitates were assessed by immunoblot. The antibodies used in each immunoblot are indicated at the right. The results were reproduced in two experiments. (C) URMT cells were infected with lentivirus encoding a GFP-MNT and 72 h later transfected with expression vectors for full length (FL) MNT or ΔHLH MNT (Figure 8C) as indicated at the top of each lane. 48 h after transfection, cell lysates were prepared and immunoprecipitated with anti-HA to pull down the transfected MNT proteins. The levels of MNT-GFP and MNT were determined by immunoblot using anti-GFP and polyclonal anti-MNT antibody. (D) HEK293T cells were co-transfected with expression vectors for MNT-GFP and expression vectors for FL MNT or ΔHLH MNT (Figure 8C) as indicated at the top of each lane. 24 h later lysates were prepared and immunoprecipitated with anti-MNT antibody. The levels of MNT-GFP and MNT were determined by immunoblot using anti-GFP and polyclonal anti-MNT antibody. The results were reproduced in two experiments. (E) Schematic summary of the interactions of MNT found in URMT (MAX-less) and URMax34 (expressing MAX when treated with Zn^{2+}).

366 cells were infected with lentiviral particles containing the GFP-MNT construct,
367 immunoprecipitated, and the lysates analysed by immunoblot with anti-GFP antibody
368 and anti-MNT antibodies. The results showed that endogenous MNT was present in the
369 immunoprecipitates with anti-GFP (*Figure 9B*). The results suggest that MNT forms
370 homodimers in human HEK293T cells and in MAX-deficient rat URMT cells. As MNT
371 dimerization in yeast two hybrid assays depends on the HLH-LZ *(Hurlin et al 1997,*
372 *Meroni et al 1997)*, we asked whether HLH was involved in the homodimerization *in vivo*.
373 We transfected the MNT mutant lacking the bHLH region (ΔbHLH MNT) (*Figure 8C*) as
374 well as the wild-type form and we carried out immunoprecipitations with anti-HA
375 antibodies which should only recognize the exogenous proteins. The immunoblot
376 analysis of the immunoprecipitates revealed that ΔbHLH MNT was unable to bind GFP-
377 MNT (*Figure 9C*). The same experiment was performed in URMT cells and the same
378 result was observed, i.e, GFP-MNT bound to wild-type MNT-HA but not to the ΔbHLH
379 form (*Figure 9D*). We conclude MNT homodimerize through the HLH domain, as
380 expected. Altogether, the results indicate that in URMT cells, MNT can form homodimers
381 or heterodimers with MLX, whereas in URMax34 (in the presence of Zn^{2+}), MNT can also
382 form heterodimers with MAX, as schematized in *Figure 9E*.
383
384
385 **DISCUSSION**
386 In this study, we report several novel findings: (i) MNT is required for optimum
387 proliferation even in the absence of MAX; (ii) in the absence of MAX, MNT expression is
388 elevated and a significant fraction localizes in the cytoplasm; (iii) MNT represses its own
389 transcription in a MAX-dependent manner; (iv) MNT is able to regulate the expression of
390 genes in the absence of MAX and (v) MNT forms homodimers in vivo. Previous reports
391 suggest that MNT functions as a "MYC buffer", curbing excessive MYC activity. For
392 instance, *in vivo* MNT knockdown impedes MYC-driven lymphomagenesis *(Campbell et*
393 *al 2017)* whereas MNT silencing leads to MYC-like phenotypes *(Hurlin et al 2003,*
394 *Nilsson et al 2004, Walker et al 2005)*. Our data are in line with this critical MNT function,
395 as they show a tight control of MNT expression by which MNT limits its own mRNA
396 expression. MNT protein levels are also under strict control in UR61 cells, as MNT cannot
397 be overexpressed at high levels upon transfection unless the proteasome is inhibited.
398 Given the relevance of MNT to modulate MYC activity and its central position between
399 the MYC-MAX and MLX-MONDO networks, the activities and regulation of MNT are a
400 key issue on MYC-dependent oncogenesis.
401 MNT expression was high in some MAX-deficient cells like the rat UR61 cells and
402 human lung carcinoma H1417 cells. The absence of MAX was in part responsible for this

403 effect because (i) MAX re-expression in UR61cells results in decreased MNT mRNA and
404 protein, and (ii) MAX overexpression in K562 cells results in MNT down-regulation
405 whereas MAX knock-down results in MNT up-regulation. The mechanism for this MAX
406 effect on MNT levels depended, at least partially, on the auto-repression of MNT
407 expression by MNT-MAX dimers. Luciferase reporter experiments showed that MNT
408 represses its own promoter (which contains two conserved E-boxes) and ChIP assays
409 showed that MNT binds to its own promoter when MAX is ectopically expressed in UR61
410 cells. In agreement with these results, significant levels of MNT localize to the cytoplasm
411 of MAX-deficient cells whereas MNT remains nuclear in MAX-expressing cells. This
412 would explain why MAX re-expression leads to a decrease in MNT levels: MNT-MAX
413 dimers would be formed to repress MNT expression in the nucleus. On the contrary, in
414 the absence of MAX, MNT is expressed at higher levels since there would be no negative
415 MNT autoregulation. The model is schematized in *Figure 10*.

416 We explored possible MAX-independent effects of MNT using the UR61 model.
417 Although originally MAX was defined as an obligate dimerization partner of MYC, work
418 carried out in the PC12 model and in *Drosophila* indicated that MYC can function in a
419 MAX-independent manner, for example in inhibition of differentiation *(Gallant 2013,*
420 *Maruyama et al 1987, Vaque et al 2008)*. MYC overexpression blocks RAS-induced
421 differentiation of UR61 cells *(Vaque et al 2008)* however, we did not detect a significant
422 effect of MNT depletion on differentiation (not shown). In contrast, depletion of MNT in
423 MAX-deficient UR61 cells impairs cell proliferation. This is the first report on a MAX-
424 independent function of a MXD protein. In contrast, in rat and mouse fibroblasts, MNT
425 knock-out leads to increased proliferation and transformation capacities *(Hurlin et al*
426 *2003, Nilsson et al 2004)*. The fact that MNT depletion impairs UR61 proliferation (in a
427 MAX-independent manner) adds complexity to the MNT-MYC functional interactions.
428 Actually, in gastric cancer high MNT expression correlates with shorter survival whereas
429 MYC overexpression has the opposite effect (http://kmplot.com/analysis/).

430 Since MNT is a transcription factor, we compared the transcriptomes of parental
431 UR61 cells versus cells with depleted MNT. Upon MNT depletion, a number of genes
432 involved in cell cycle progression and DNA damage response were downregulated in
433 cells with and without MAX. This is concordant with the decrease in proliferation exerted
434 by MNT silencing in UR61. It is open to discussion how MNT regulates genes in the
435 absence of MAX. MNT can form heterodimers with the HLH protein MLX *(Cairo et al*
436 *2001, Meroni et al 2000)* and we have confirmed the ability of MNT to bind MLX in UR61
437 cells, but when MAX is expressed, the dimers MNT-MAX are favoured versus MNT-MLX.
438 As a relevant fraction of MLX is cytoplasmic and we have shown that MNT and MLX also

interact in the cytoplasm, this interaction could help to explain the increase in cytoplasmic MNT observed in MAX-depleted cells. The model is depicted in the *Figure 10*. Moreover, we have shown that MNT homodimerizes in UR61 cells, and therefore it is likely that MNT regulates genes as a homodimer. Further work is required to clarify this point. The results reported here show a strict autoregulation of MNT, supporting a pivotal role of MNT in the control of cell proliferation even in the absence of MAX. Moreover, we showed that MNT has activities in the absence of MAX. Given that MNT participates in both the MAX-MYC and MLX-MONDO networks, the regulation of MNT is a relevant issue in cell biology and in tumor development promoted by MYC.

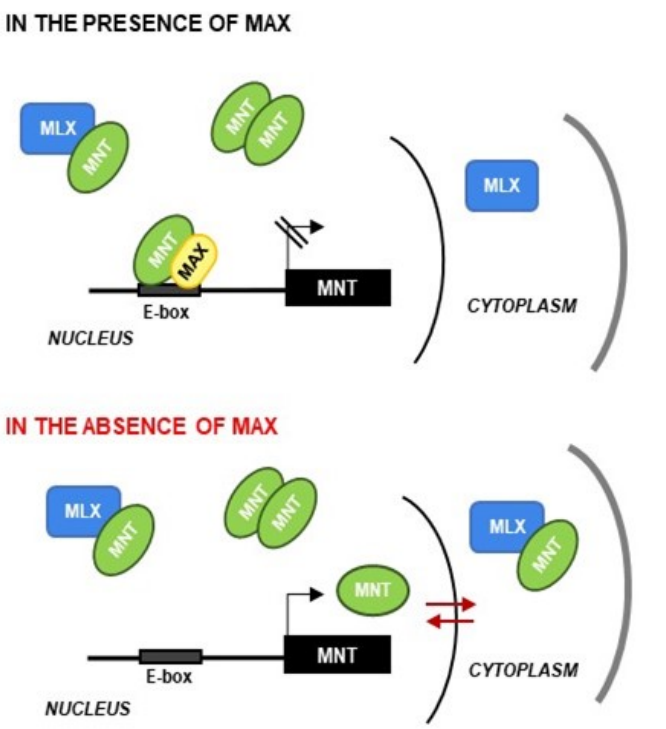

Figure 10. Model of MNT fates depending on MAX. In MAX-expressing cells, most of the MNT is retained in the cell nucleus where it limits its own expression. In MAX-deficient cells as UR61, MNT is distributed in nucleus and cytoplasm and is unable to bind the promoter and regulate its transcriptional activity. The model includes the presence of MNT-MNT homodimers and the interaction MNT-MLX in the cytoplasm, which might be responsible for the MNT partial localization in the cytoplasm in MAX-deficient cells.

MATERIALS AND METHODS

Cell lines and transfections

Cell lines were obtained from ATCC and grown in either RPMI-1640 or DMEM (Lonza) supplemented with 10% fetal bovine serum (Lonza), 150 µg/ml of gentamicin and 2 µg/ml of ciprofloxacin. To generate the URMT and URMax34 cell line, UR61 cells *(Guerrero et al 1988)* were electroporated (260 V, 1 mFa, BioRad apparatus) with a pHeBo-MT or pHeBo-MT-Max vector which carries a human MAX cDNA under the control of metallothionein promoter *(Canelles et al 1997)*. Cells were selected with 0.2 mg/ml of hygromycin (Life Technologies) and cell clones were isolated by limiting dilution Transient transfections were carried out using the Ingenio Electroporation solution (Mirus) in an Amaxa nucleofector. The cells were transfected or transduced with expression vectors for MAX (pCEFL-MAX*(Mauleon et al 2004)*, MLX (β isoform, (pMS18-

475 MLX,*(Billin et al 1999)*, human MNT (pCMVSport6-MNT, Origene Technologies), MNT-
476 Flag (human MNT with FLAG at the C-ter lentiviral Lv158 vector Genecopoeia), MNT-
477 GFP (human MNT with GFP at the N-ter, lentiviral Lv103 vector Genecopiea,), FL MNT-
478 HA (full-length murine MNT tagged at the C-ter with hemagglutinin epitope, HA), ΔHLH
479 MNT-HA (murine MNT carrying a deletion of amino acids 221-272 amino acids and
480 tagged with HA) (both in pcDNA3 with the zeocin resistance gene inserted), short-hairpin
481 human MNT-1 (shMNT-1, pLKO-shMNT from Sigma Mission, TRCN0000085733), or
482 MNT-2 (shMNT-2, pLKO-shMNT from Sigma Mission, TRCN0000235815), siRNA for
483 human MAX (Sigma, SASI_Hs01_00011941).
484

485 **Immunoblot and immunoprecipitation**

486 Cell lysis, immunoblots and immunoprecipitations were performed as described.*(Garcia-*
487 *Sanz et al 2014)* .The antibodies used are described in *Supplementary File 1.*

488 **Luciferase reporters and assays**

489 To generate the 850MNT-luc, 220MNT-luc, 570MNT-luc reporter vectors, two pair of
490 primers were designed for each construct (*Supplementary File 2*), targeting sequences
491 of the human genome corresponding to 850 bp upstream the transcription start site
492 (TSS) of *MNT* gene. The amplified DNA was inserted into the pBV-luc reporter vector at
493 the EcoRV and HindIII sites *(He et al 1998)*. The sequence of MNT promoter was from
494 the UCSC genome browser (http://genome.ucsc.edu/; GRCh37/hg19). Cells were
495 transfected with jetPEI reagent (Polyplus) and luciferase assays were performed as
496 described *(Garcia-Sanz et al 2014)*.
497

498 **Cell proliferation and cell cycle analysis**

499 Cell proliferation was monitored with a cell counter (NucleoCounter NC-100,
500 Chemometec) or a cytometer (Guava PCA, Merck Millipore). For the clonogenic assays,
501 1-2 x 10^6 cells/ml were seeded in a 6-well or 60 mm plate after transfection by
502 electroporation. 48 h post-transfection, cells were selected with puromycin at 0.2-0.5
503 µg/ml final concentration. After 8-17 days the cells were stained with crystal violet and
504 the dye measured by absorbance at 595 nm as described *(Ferrandiz et al 2009)*. To
505 determine the sugG0-G1 population, cells were transfected and 7 days post-transfection
506 the DNA concentration was analyzed by propidium iodide staining and flow cytometry
507 as described *(Albajar et al 2011)*.
508
509

510 **RNA analysis**

511 For qPCR, total RNA was isolated using the TRI Reagent® Solution (Invitrogen). cDNA
512 was generated by reverse transcription (RT) using the iScript (Bio-Rad). Quantitative
513 polymerase chain reaction (qPCR) was performed with specific primers (*Supplementary*
514 *File 2*) using the iTaq™ Universal SYBR® Green Supermix (Bio-Rad) and CFX
515 ConnectTM Real-Time PCR Detection System (Bio-Rad). RNA was converted into cDNA
516 and analysed as described *(Bretones et al 2011)*. Levels of mRNA were normalized
517 against actin and RPS14 mRNA levels. For RNA-seq, total RNA was isolated with the
518 RNeasy kit (Qiagen) from two independent experiments of MNT silencing in URMT and
519 URMax34 cells, both treated with 100 μM $ZnSO_4$ for 24 h. mRNA libraries were prepared
520 using the Illumina TruSeq RNA Sample Prep Kit v2 (kit RS-122-2002, Illumina). A
521 minimum of 40 million 50 bases single-end reads per sample were obtained. Tophat
522 algorithm *(Trapnell et al 2009)* was used to align the data using a set of gene model
523 annotations and/or known transcripts of rat genome (rn4) obtained from RefSeq
524 database. Cufflinks software *(Trapnell et al 2010)* was run to estimate transcripts
525 abundances represented in RPKM units (reads per kilobase per million reads) as
526 described (Mortazavi et al 2008). The gene expression of the genes are represented as
527 RPKM values (*Figure 8 –Supplement 2 to 5)*.

528

529 **Chromatin immunoprecipitation**

530 Fractionation of total cell extracts into cytoplasmic and nuclear fractions and chromatin
531 immunoprecipitation (ChIP) were performed essentially as described *(Garcia-Sanz et al*
532 *2014)*. Immunoprecipitated DNA was purified with the QIAquick PCR Purification
533 Kit (Qiagen) and analysed by qPCR. The antibodies and primers used are described in
534 *Supplementary Files 1 and 2,* respectively.

535

536 **Nuclear/cytoplasmic fractionation**

537 Cytoplasmic and nuclear extracts were prepared essentially as described *(Conacci-*
538 *Sorrell et al 2010)*. The hypotonic buffer to lyse cells was 10 mM HEPES pH 7, 10 mM
539 KCl, 0.25 mM EDTA pH 8, 0.125 mM EGTA pH 8, 0.5 mM spermidin, 0.1% NP40, 1 mM
540 DTT and proteases inhibitors The hypertonic buffer for nuclear extracts was 20 mM
541 HEPES, 400 mM NaCl, 0.25 mM EDTA, 1.5 mM $MgCl_2$, 0.5 mM DTT and proteases
542 inhibitors.

543

544

545

546 **Statistical analysis**

547 Student's t-test was used to evaluate the significance of differences between control and
548 experimental groups. A p-value of less than 0.05 was considered as significant. The
549 threshold for expression changes in the RNA-seq analysis was set as log2(RPKM fold
550 change) ≥ 0.7 or ≤ -0.7 and a p-value <0.1.

551

552 **Bioinformatic analysis**

553 Genomic sequences of 1000 bp upstream TSS of human, mouse and rat MNT genes
554 were obtained from *H. sapiens* (GRCh37/hg19), *M. musculus* (GRCm38/mm10) and *R.*
555 *norvegicus* (RGSC 5.0/rn5) assemblies. For the ChIP-seq ENCODE analysis, the data
556 for MAX, MYC and MXI1 was obtained for the indicated cell lines. The SYDH ENCODE
557 project was chosen for representation of the binding peaks in the promoter of the human
558 MNT gene. The sequences corresponding to those peaks were analysed confirming the
559 presence of the E-boxes identified in the human MNT promoter

560

561 **Source data**: the RNA-seq data is loaded in the European Nucleotide Archive with the
562 accession number PRJEB23604

563

564 **ACKNOWLEDGEMENTS**

565 We are grateful to Montserrat Sánchez-Céspedes and Don Ayer for cell lines and
566 constructs, Maralice Conacci-Sorrel for comments on the manuscript, and Sandra
567 Zunzunegui and Maria Aramburu for technical help.

568

569 **FUNDING**

570 The work was supported by grant SAF2014-53526-R from MINECO, Spanish
571 Government, to JL and MDD (partially funded by FEDER program from European Union)
572 RNE is supported by grant CA57138/CA/NCI from National Institutes of Health. PJH is
573 supported by grants from Shriners Hospitals for Children. MCL-N and JL-P were
574 recipients of F.P.U. fellowships from Spanish Government.

575

576 **CONFLICT OF INTEREST**

577 The authors declare no conflict of interests

578

579 **AUTHOR ORCID**

580 Javier León, https://orcid.org/0000-0001-5803-0112

581

582

583

584 **REFERENCES**

585 Albajar M, Gomez-Casares MT, Llorca J, Mauleon I, Vaque JP, Acosta JC, Bermudez
586 A, Donato N, Delgado MD, Leon J. 2011. MYC in chronic myeloid leukemia:
587 induction of aberrant DNA synthesis and association with poor response to
588 imatinib. *Mol Cancer Res* **9**: 564-76
589 Billin AN, Eilers AL, Coulter KL, Logan JS, Ayer DE. 2000. MondoA, a novel basic
590 helix-loop-helix-leucine zipper transcriptional activator that constitutes a positive
591 branch of a max-like network. *Mol Cell Biol* **20**: 8845-54
592 Billin AN, Eilers AL, Queva C, Ayer DE. 1999. Mlx, a novel Max-like BHLHZip protein
593 that interacts with the Max network of transcription factors. *J Biol Chem* **274**:
594 36344-50
595 Bretones G, Acosta JC, Caraballo JM, Ferrandiz N, Gomez-Casares MT, Albajar M,
596 Blanco R, Ruiz P, Hung WC, Albero MP, Perez-Roger I, Leon J. 2011. SKP2
597 oncogene is a direct MYC target gene and MYC down-regulates p27(KIP1)
598 through SKP2 in human leukemia cells. *J Biol Chem* **286**: 9815-25
599 Cairo S, Merla G, Urbinati F, Ballabio A, Reymond A. 2001. WBSCR14, a gene
600 mapping to the Williams--Beuren syndrome deleted region, is a new member of
601 the Mlx transcription factor network. *Hum Mol Genet* **10**: 617-27
602 Campbell KJ, Vandenberg CJ, Anstee NS, Hurlin PJ, Cory S. 2017. Mnt modulates
603 Myc-driven lymphomagenesis. *Cell Death Differ* **24**: 2117-26
604 Canelles M, Delgado MD, Hyland KM, Lerga A, Richard C, Dang CV, Leon J. 1997.
605 Max and inhibitory c-Myc mutants induce erythroid differentiation and resistance
606 to apoptosis in human myeloid leukemia cells. *Oncogene* **14**: 1315-27
607 Conacci-Sorrell M, McFerrin L, Eisenman RN. 2014. An Overview of MYC and Its
608 Interactome. *Cold Spring Harb Perspect Med* **4**: 1-24
609 Conacci-Sorrell M, Ngouenet C, Eisenman RN. 2010. Myc-nick: a cytoplasmic
610 cleavage product of Myc that promotes alpha-tubulin acetylation and cell
611 differentiation. *Cell* **142**: 480-93
612 Dang CV. 2012. MYC on the path to cancer. *Cell* **149**: 22-35
613 Dezfouli S, Bakke A, Huang J, Wynshaw-Boris A, Hurlin PJ. 2006. Inflammatory
614 disease and lymphomagenesis caused by deletion of the Myc antagonist Mnt in
615 T cells. *Mol Cell Biol* **26**: 2080-92
616 Diolaiti D, McFerrin L, Carroll PA, Eisenman RN. 2015. Functional interactions among
617 members of the MAX and MLX transcriptional network during oncogenesis.
618 *Biochim Biophys Acta* **1849**: 484-500
619 Ferrandiz N, Martin-Perez J, Blanco R, Donertas D, Weber A, Eilers M, Dotto P,
620 Delgado MD, Leon J. 2009. HCT116 cells deficient in p21(Waf1) are
621 hypersensitive to tyrosine kinase inhibitors and adriamycin through a
622 mechanism unrelated to p21 and dependent on p53. *DNA Repair* **8**: 390-9
623 Foley KP, McArthur GA, Queva C, Hurlin PJ, Soriano P, Eisenman RN. 1998. Targeted
624 disruption of the MYC antagonist MAD1 inhibits cell cycle exit during
625 granulocyte differentiation. *EMBO J* **17**: 774-85
626 Gallant P. 2013. Myc function in Drosophila. *Cold Spring Harb Perspect Med* **3**:
627 a014324
628 Garcia-Sanz P, Quintanilla A, Lafita MC, Moreno-Bueno G, Garcia-Gutierrez L, Tabor
629 V, Varela I, Shiio Y, Larsson LG, Portillo F, Leon J. 2014. Sin3b interacts with
630 myc and decreases myc levels. *J Biol Chem* **289**: 22221-36
631 Guerrero I, Pellicer A, Burstein DE. 1988. Dissociation of c-fos from ODC expression
632 and neuronal differentiation in a PC12 subline stably transfected with an
633 inducible N-ras oncogene. *Biochem Biophys Res Commun* **150**: 1185-92
634 He TC, Sparks AB, Rago C, Hermeking H, Zawel L, da Costa LT, Morin PJ, Vogelstein
635 B, Kinzler KW. 1998. Identification of c-MYC as a target of the APC pathway.
636 *Science* **281**: 1509-12

637 Hopewell R, Ziff EB. 1995. The nerve growth factor-responsive PC12 cell line does not
638 express the Myc dimerization partner Max. *Mol Cell Biol* **15**: 3470-8
639 Hurlin PJ, Queva C, Eisenman RN. 1997. Mnt, a novel Max-interacting protein is
640 coexpressed with Myc in proliferating cells and mediates repression at Myc
641 binding sites. *Genes Dev* **11**: 44-58.
642 Hurlin PJ, Zhou ZQ, Toyo-oka K, Ota S, Walker WL, Hirotsune S, Wynshaw-Boris A.
643 2003. Deletion of Mnt leads to disrupted cell cycle control and tumorigenesis.
644 *EMBO J* **22**: 4584-96
645 Lafita-Navarro MC, Blanco R, Mata-Garrido J, Liano-Pons J, Tapia O, Garcia-Gutierrez
646 L, Garcia-Alegria E, Berciano MT, Lafarga M, Leon J. 2016. MXD1 localizes in
647 the nucleolus, binds UBF and impairs rRNA synthesis. *Oncotarget* **7**: 69536-48
648 Maruyama K, Schiavi SC, Huse W, Johnson GL, Ruley HE. 1987. myc and E1A
649 oncogenes alter the responses of PC12 cells to nerve growth factor and block
650 differentiation. *Oncogene* **1**: 361-7
651 Mauleon I, Lombard MN, Munoz-Alonso MJ, Canelles M, Leon J. 2004. Kinetics of
652 myc-max-mad gene expression during hepatocyte proliferation in vivo:
653 Differential regulation of mad family and stress-mediated induction of c-myc.
654 *Mol Carcinog* **39**: 85-90
655 Meroni G, Cairo S, Merla G, Messali S, Brent R, Ballabio A, Reymond A. 2000. Mlx, a
656 new Max-like bHLHZip family member: the center stage of a novel transcription
657 factors regulatory pathway? *Oncogene* **19**: 3266-77
658 Meroni G, Reymond A, Alcalay M, Borsani G, Tanigami A, Tonlorenzi R, Nigro CL,
659 Messali S, Zollo M, Ledbetter DH, Brent R, Ballabio A, Carrozzo R. 1997. Rox,
660 a novel bHLHZip protein expressed in quiescent cells that heterodimerizes with
661 Max, binds a non-canonical E box and acts as a transcriptional repressor.
662 *EMBO J* **16**: 2892-906.
663 Mortazavi A, Williams BA, McCue K, Schaeffer L, Wold B. 2008. Mapping and
664 quantifying mammalian transcriptomes by RNA-Seq. *Nat Methods* **5**: 621-8
665 Nilsson JA, Maclean KH, Keller UB, Pendeville H, Baudino TA, Cleveland JL. 2004.
666 Mnt loss triggers Myc transcription targets, proliferation, apoptosis, and
667 transformation. *Mol Cell Biol* **24**: 1560-9
668 Popov N, Wahlstrom T, Hurlin PJ, Henriksson M. 2005. Mnt transcriptional repressor is
669 functionally regulated during cell cycle progression. *Oncogene* **24**: 8326-37
670 Queva C, McArthur GA, Ramos LS, Eisenman RN. 1999. Dwarfism and dysregulated
671 proliferation in mice overexpressing the MYC antagonist MAD1. *Cell Growth*
672 *Differ* **10**: 785-96
673 Romero OA, Torres-Diz M, Pros E, Savola S, Gomez A, Moran S, Saez C, Iwakawa R,
674 Villanueva A, Montuenga LM, Kohno T, Yokota J, Sanchez-Cespedes M. 2014.
675 MAX inactivation in small cell lung cancer disrupts MYC-SWI/SNF programs
676 and is synthetic lethal with BRG1. *Cancer Discov* **4**: 292-303
677 Schreiber-Agus N, DePinho RA. 1998. Repression by the Mad(Mxi1)-Sin3 complex.
678 *Bioessays* **20**: 808-18
679 Terragni J, Nayak G, Banerjee S, Medrano JL, Graham JR, Brennan JF, Sepulveda S,
680 Cooper GM. 2011. The E-box binding factors Max/Mnt, MITF, and USF1 act
681 coordinately with FoxO to regulate expression of proapoptotic and cell cycle
682 control genes by phosphatidylinositol 3-kinase/Akt/glycogen synthase kinase 3
683 signaling. *J Biol Chem* **286**: 36215-27
684 Toyo-oka K, Hirotsune S, Gambello MJ, Zhou ZQ, Olson L, Rosenfeld MG, Eisenman
685 R, Hurlin P, Wynshaw-Boris A. 2004. Loss of the Max-interacting protein Mnt in
686 mice results in decreased viability, defective embryonic growth and craniofacial
687 defects: relevance to Miller-Dieker syndrome. *Hum Mol Genet* **13**: 1057-67
688 Trapnell C, Pachter L, Salzberg SL. 2009. TopHat: discovering splice junctions with
689 RNA-Seq. *Bioinformatics* **25**: 1105-11
690 Trapnell C, Williams BA, Pertea G, Mortazavi A, Kwan G, van Baren MJ, Salzberg SL,
691 Wold BJ, Pachter L. 2010. Transcript assembly and quantification by RNA-Seq

692 reveals unannotated transcripts and isoform switching during cell differentiation.
693 *Nat Biotechnol* **28**: 511-5
694 Vaque JP, Fernandez-Garcia B, Garcia-Sanz P, Ferrandiz N, Bretones G, Calvo F,
695 Crespo P, Marin MC, Leon J. 2008. c-Myc inhibits Ras-mediated differentiation
696 of pheochromocytoma cells by blocking c-Jun up-regulation. *Mol Cancer Res* **6**:
697 325-39
698 Walker W, Zhou ZQ, Ota S, Wynshaw-Boris A, Hurlin PJ. 2005. Mnt-Max to Myc-Max
699 complex switching regulates cell cycle entry. *J Cell Biol* **169**: 405-13
700 Yang G, Hurlin PJ. 2017. MNT and Emerging Concepts of MNT-MYC Antagonism.
701 Genes 8: pii: E83

702